

Designed Beta-Turn Mimic Based on the Allylic-Strain Concept: Evaluation of Structural and Biological Features by Incorporation into a Cyclic RGD Peptide (Cyclo(-L-arginylglycyl-L- α -aspartyl-))

by Martin Sukopp^a), Luciana Marinelli^a), Markus Heller^a), Trixi Brandl^b), Simon L. Goodman^c),
Reinhard W. Hoffmann^b), and Horst Kessler^{*a})

^a) Institut für Organische Chemie und Biochemie, Technische Universität München, Lichtenbergstr. 4,
D-85747 Garching (fax: +49-089-289-13210)

^b) Fachbereich Chemie der Philipps-Universität Marburg, Hans-Meerwein-Strasse, D-35032 Marburg

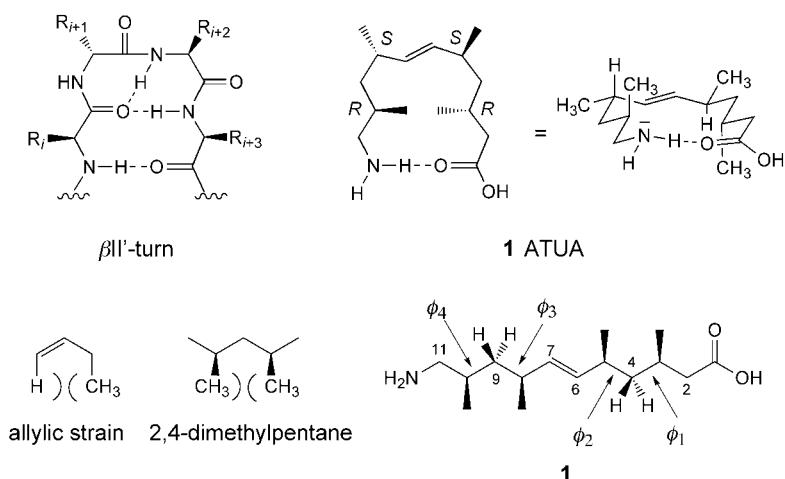
^c) Department of Medicinal Chemistry, Merck KGaA, Frankfurter Strasse 250, D-64271 Darmstadt

Dedicated to Prof. Dr. D. Seebach on the occasion of his 65th birthday

The (3*R*,5*S*,6*E*,8*S*,10*R*)-11-amino-3,5,8,10-tetramethylundec-6-enoic acid (ATUA; **1**), which was designed as a β II'-turn mimic according to the concepts of allylic strain and 2,4-dimethylpentane units, was incorporated into a cyclic RGD peptide. The three-dimensional structure of cyclo(-RGD-ATUA-) (= cyclo(-Arg-Gly-Asp-ATUA-)) **4** in H₂O was determined by NMR techniques, distance geometry calculations and molecular-dynamics simulations. The RGD sequence of **4** shows high conformational flexibility but some preference for an extended conformation. The structural features of the RGD sequence of **4** were compared with the RGD moiety of cyclo(-RGDfV-) (= cyclo(-Arg-Gly-Asp-D-Phe-Val-)). In contrast to cyclo(-RGDfV-), which is a highly active *av* β 3 antagonist and selective against α IIb β 3, cyclo(-RGD-ATUA-) shows a lower activity and selectivity. The structure of the ATUA residue in the cyclic peptide resembles a β II'-turn-like conformation. Its middle part, adjacent to the C=C bond, strongly prefers the designed and desired structure.

1. Introduction. – The structural unit of β -turns is found in many proteins and bioactive peptides [1]. It functions to reverse the direction of peptide strands ('hairpin structure') as well as a recognition element in exposed loops. Since it contains only a small number of atoms, β -turn mimics have been a widely sought synthetic target in the last decade. Actually, the aims of research in this field are to stabilize the conformation of β -turns by cyclization and to achieve higher metabolic stability through the use of rigid, non-peptidic molecules [2–7].

The (3*R*,5*S*,6*E*,8*S*,10*R*)-11-amino-3,5,8,10-tetramethylundec-6-enoic acid (ATUA; **1**), which was used in this study, is also based on the idea of limited conformational freedom. In contrast to most other β -turn mimics, consisting of mono- or bicyclic structures, ATUA is a linear molecule. The design and synthesis of this kind of β -turn mimic was described earlier [8]. Suffice is to say that the mimic was designed according to two concepts: the allylic strain [9][10] and 2,4-dimethylpentane units [11] that are found in polyketide natural products. The (*E*)-alkene unit in the middle of ATUA substitutes the amide bond that is present in natural peptides. The turn mimic, which represents a chain of four amino acids, is supposed to adopt a β II' hairpin-like arrangement.



The structure of the bis-amide of the ATUA enantiomer¹⁾ was previously determined by NMR and IR spectroscopy and by MM3 calculations [8]. It could be shown that the strongest populated conformation of the enantiomer of ATUA adopts a β II'-turn-like conformation. The reasons for this finding are, as mentioned before, the minimization of the allylic strain between the C=C bond and the adjacent Me groups, and the steric hindrance of the four Me groups. Further stabilization results from the H-bond between the NH and CO of the β -turn mimic, as shown by IR and NMR experiments. This, of course, depends strongly on the solvent used.

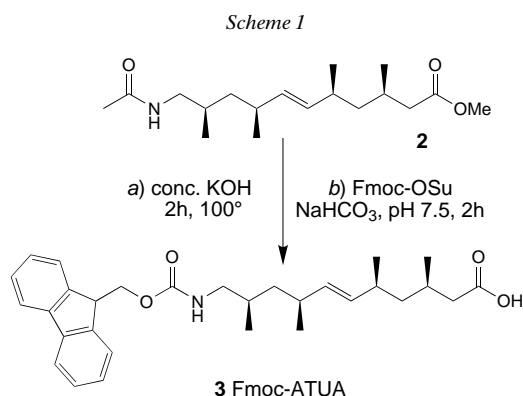
Frequently, β -turn mimics are incorporated into the peptide chain of cyclic peptides to obtain rigidified structures with the turn mimic in the desired position. However, the aim was not achieved in every case. The mimic has to compete with the position and chirality of the other amino acids in the cycle for the position of the β -turn [12], *e.g.* Gly often acts as a D-amino acid and, hence, is found in the $i + 1$ position of a β II'-turn [13]. The overall structure then decides whether one or two β -turns are allowed in such a cycle and which is the preferred one in cycles that allow only one β -turn.

To establish whether ATUA (**1**) is able to adopt a β II'-turn conformation in cyclic peptides, it was incorporated into a cyclic RGD peptide (cyclo(-RGA-) = (cyclo(-Arg-Gly-Asp-))). We have chosen the RGD peptides because they are of biological relevance, and also because there is a large amount of information already available about conformation and activity in cyclic RGD peptides. In the past, several known rigid building blocks were incorporated into cyclic penta- and hexapeptides containing the RGD sequence [12]. Recently, structurally modified sugar amino acids were also used in this context [14]. In this study, we have chosen the cyclo(-RGDfV-) (= cyclo(-Arg-Gly-Asp-D-Phe-Val-)) as a lead compound because it binds selectively and with high affinity to the $\alpha v\beta 3$ integrin cell receptor (vitronectin receptor) [15–18]. Integrins

¹⁾ By inverting the configuration at the stereogenic centers of ATUA, the conformation of the turn switches from β II' to its mirror image β II. This was shown by molecular-dynamic calculations with a CVFF force field.

are located at the cell surface of a number of different cell types and play a major role in cell-matrix interactions and in tumor genesis [19–24]²⁾. This aroused pharmaceutical interest in $\alpha v\beta 3$ antagonists, especially with regard to blocking tumor-induced angiogenesis [26][27]. The analogue with the *N*-methylated peptide bond cyclo(-RGD-N(Me)V-) is in phase II clinical trials as anticancer drug (*Cilengitide*, EMD 121974) [28]. In the present work, the original sequence of cyclo(-RGDfV-) was modified by replacing the D-Phe-Val (=fV) moiety with ATUA, because it is well-known that the D-Phe-Val moiety arranges in a β II'-turn [18], leading to cyclo(-RGD-ATUA-) (**4**). Here, we compare the structural features of the RGD moieties of both cyclopeptides. In addition, we make a comparison of the ATUA moiety with an ideal β II'-turn.

2. Results and Discussion. – 2.1. *Synthesis.* One intermediate of the synthesis of compound **4** is the *N*-acetyl methyl ester **2** [8], which was converted to the Fmoc-protected amino acid **3** by reflux in concentrated KOH solution and subsequent protection of the N-terminus with *N*-[(9*H*-fluoren-9-ylmethoxy)carbonyl]oxy)succinimide (Fmoc-OSu) at pH 7.5 in a one-pot reaction sequence (*Scheme 1*).

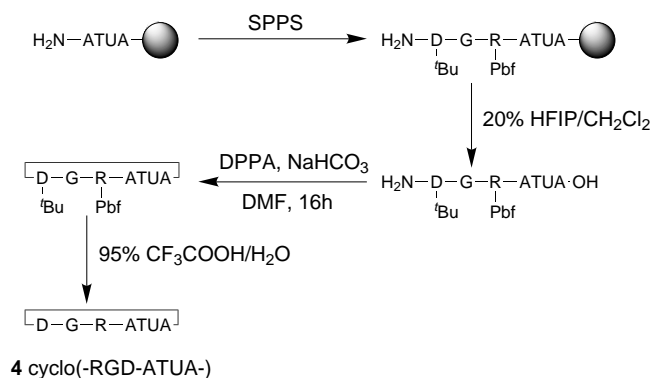


The Fmoc-ATUA **3** was used in solid-phase peptide synthesis (SPPS) by standard Fmoc strategy to prepare the cyclic RGD peptide; thereby, **3** was the first amino acid to be immobilized on the trityl chloride polystyrol (TCP) resin (*Scheme 2*). After coupling of the RGD sequence and cleavage from the resin with 1,1,1,3,3,3-hexafluoropropan-2-ol (HFIP), cyclization in solution with diphenoxyphosphoryl azide (DPPA) was performed. Final deprotection was achieved with CF₃COOH and a scavenger (triisopropylsilane). Purification by reversed-phase HPLC yielded peptide **4**, which was > 98% pure.

2.2. *Biological Activity.* The biological activity and selectivity of **4** was tested as described earlier (*Table 1*) [29]. The low activity of **4** (IC_{50} , 1 μ M) resembles that of the linear peptide GRGDSPK. The high activity of cyclo(-RGDfV-) (IC_{50} , 2 nM) towards the vitronectin receptor $\alpha v\beta 3$ and the good selectivity between $\alpha v\beta 3$ and the platelet receptor $\alpha IIb\beta 3$ (IC_{50} , 850 nM) is based on its kink about Gly [16]. The D-Phe residue occupies the $i + 1$ position of the β II'-turn. From the biological point of view, it seems

²⁾ Recently, the crystal structure of the $\alpha v\beta 3$ integrin with a RGD ligand was published [25].

Scheme 2

Table 1. IC_{50} Values of RGD Peptides

Peptide	$\alpha v \beta 3$ IC_{50} [nM]	$\alpha \text{IIb} \beta 3$ IC_{50} [nM]
GRGDSPK	1000	$> 10^4$
cyclo(RGDfV)	2	850
cyclo(RGD-ATUA-) (4)	1000	1000
cyclo(RGDf-N(Me)-V-)	0.6	876
cyclo(- β -SAA(Bn) ₃ -RGD-) ^a	25	13.4

^a) The structure of cyclo(- β -SAA(Bn)₃-RGD-) was described earlier [14]. SAA = sugar amino acid.

that compound **4** is quite flexible, and the RGD sequence might be only partly arranged in a kink about Gly.

2.3. Conformational Analysis. The three-dimensional structure of **4** in H₂O was determined by NMR spectroscopy, metric matrix distance geometry (DG) calculations, and molecular-dynamics (MD) simulations. Assignment of the ¹H- and ¹³C-NMR resonances could be obtained (Table 2). The proton-proton distances were calculated from a ROESY experiment measured with a mixing time of 200 ms. The ROESY cross-peak volumes were converted into distances *via* the 2.6 Å reference from NH of ATUA and H-C(α) of Asp (by the isolated two-spin approximation). The distances were adjusted by $\pm 10\%$ to produce the upper and lower distance restraints. The prochiral methylene protons of CH₂(4) and CH₂(9) were stereospecifically assigned on the basis of ROE values and ³J(H,H) coupling constants. Additional stereospecific assignments, as in the case of the Arg and Asp side chains, were not possible due to signal overlap and small differentiation in spectral parameters. The ROE intensities regarding Gly H-C(α) were not used as distance restraints in the calculations because they seem to be averaged over the NMR time scale³). The starting geometry for the MD simulation was obtained by DG with a modified version of the DISGEO program [30–32] taken from 28 informative proton-proton distances and the two ³J(NH, H-C(α)) coupling

³) Initial calculations considering both Gly H-C(α) distances from the two adjacent NH yielded unreasonable structures and mutually exclusive distances.

Table 2. ^1H - and ^{13}C -NMR Chemical Shifts of Cyclopeptide **4** in H_2O at 300K and Temperature Coefficients for the Amide Protons

Residue	$\delta(\text{H})$ [ppm]					
	NH	H–C(α) or CH ₂ (α)	CH ₂ (β)	CH ₂ (γ)	CH ₂ (δ)	H–N(ϵ)
Arg	8.22 (9.5 ^a)	4.25	1.78, 1.88	1.70	3.24	7.31
Gly	8.50 (5.8 ^a)	3.86, 4.02	–	–	–	–
Asp	8.17 (3.3 ^a)	4.63	2.80	–	–	–
ATUA	7.70 (5.9 ^a) (NH)	3.12, 2.97 (CH ₂ (11)) 5.19 (H–(6)) 0.81 (Me–C(3)) 0.95 (Me–C(8))	1.65 (H–C(10)) 2.18 (H–C(5)) 0.92 (Me–C(5)) 0.84 (Me–C(10))	1.01 (H _{proR} –C(9)) 1.27 (H _{proS} –C(9)) 1.11 (H _{proR} –C(4)) 1.26 (H _{proS} –C(4))	2.21 (H–(8)) 1.90 (H–C(3))	5.16 (H–C(7)) 2.06, 2.26 (CH ₂ (2))
$\delta(\text{C})$ [ppm]						
	C(α)	C(β)	C(γ)	C(δ)		
Arg	56.6	30.5	27.3	43.4		
Gly	45.9	–	–	–		
Asp	54.0	39.6	178.5	–		
ATUA	47.1 (C(2)) 118.8 (C(6)) 33.5 (C(10)) 20.4 (Me–C(3))	31.9 (C(3)) 118.9 (C(7)) 49.1 (C(11)) 24.6 (Me–C(5))	46.5 (C(4)) 36.8 (C(8)) 24.8 (Me–C(8))	36.8 (C(5)) 43.6 (C(9)) 18.4 (Me–C(10))		

^a) The temperature coefficients are given in $-\Delta\delta/\Delta T$ [ppb/K] (parts per billion per K).

constants for Arg and Asp residues (6.2 Hz and 7.7 Hz, resp.). The structure with the smallest total error was subjected to further refinement. The MD simulations were carried out in explicit H_2O . The ROE restraints were used for 150 ps of the simulation (restrained MD = rMD) and then removed (free MD = fMD) for another 150 ps.

Analysis of the trajectory of the molecular dynamics shows that the middle part of the ATUA, ranging from C(3) to C(10), is conformationally stable and adopts the predicted $\beta\text{II}'$ -turn-like arrangement. The conformational preference and the symmetry of this part of the ATUA is confirmed by some vicinal $^3J(\text{H},\text{H})$ coupling constants. The $^3J(\text{H},\text{H})$ -coupling constants of H_{proR}–C(4) and H_{proR}–C(9) with their neighbors (H–C(3) and H–C(5) and H–C(8) and H–C(10)), resp.) are 3.5 and 10.8 Hz and 11.4 and 3.9 Hz, respectively⁴). This means that the dihedral angles for the protons H_{proR}–C(4) and H_{proR}–C(9) are nearly identical ($\Phi_1 = \Phi_4$ and $\Phi_2 = \Phi_3$ (see *Formula 1*)). To compare calculated with experimental coupling constants during rMD simulations, the $^3J(\text{H},\text{H})$ were obtained by averaging the J values of each individual conformation over the trajectory. The calculated coupling constants for the angles Φ_1 , Φ_2 , Φ_3 , and Φ_4 are 2.3, 11.9, 11.8, and 3.9 Hz, respectively⁵). Therefore, the simulation is in very good agreement with the experimental values.

For the averaged and minimized structure from rMD, superposition of the ATUA backbone atoms from C(3) to C(10) (middle part of ATUA) and the corresponding

⁴) Similar coupling constants can be measured from the same protons of the ATUA hydrochloride in H_2O (data not shown). This compound seems to exhibit stability and symmetry even when not incorporated into a cyclic molecule.

⁵) Empirical Karplus equation: $^3J = 6.4 - 0.8 \cos(\Phi) + 4.96 \cos(2\Phi)$ [33][34].

atoms in the ideal β II'-turn fit with a root-mean-square deviation (r.m.s.d.) value of 0.49 Å (Fig. 1). On the other hand, the superposition of all the backbone atoms in the ATUA and the corresponding atoms in the ideal turn led to a r.m.s.d. value of 1.0 Å. As shown in Fig. 1, with respect to the ideal turn, the ATUA widens in its terminal parts, losing completely the H-bond that was partly observed in CCl₄ solution of the free ATUA [8].

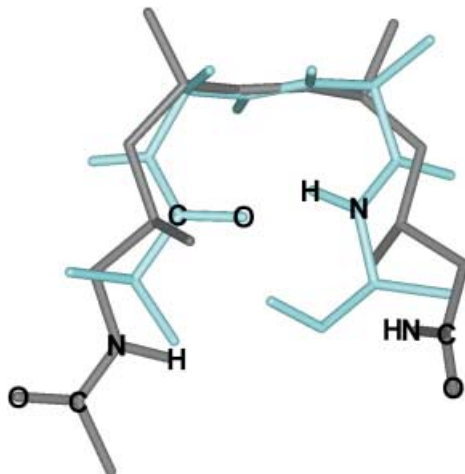


Fig. 1. Superposition of an ideal β II'-turn (gray) with the ATUA moiety (black) of the cyclo(-RGD-ATUA-). Only backbone atoms from C(3) to C(10) of ATUA and the corresponding atoms in the ideal turn are considered for the r.m.s.d. calculation.

Analysis of the MD trajectories of **4** shows that the highest conformational variability is exhibited by the RGD sequence. The pharmacophoric moiety can be arranged in three turns: two γ_i -turns with Arg and Asp at position $i + 1$ and one γ -turn with Gly at position $i + 1$ (Fig. 2). According to the corresponding H-bonds, the turns are populated 21, 13, and 17% during the rMD (Table 3). The temperature coefficients of the NH protons, which are often considered a measure of the solvent accessibility of amide protons, are shown in Table 2.

Table 3. Population of the H-Bonds of **4** in H₂O during the Restrained MD Simulation^{a)}

Donor	Acceptor	Population [%]
Gly NH	ATUA CO	21
Asp NH	Arg CO	17
ATUA NH	Gly CO	13
ATUA NH	ATUA CO	0
ATUA NH	Arg CO	0

^{a)} H-Bonds are defined by a distance $D_{D,A}$ between the donor and acceptor of < 2.7 Å and an angle δ between the vectors CO and NH of $180 \pm 70^\circ$.

During both dynamic calculations (rMD, fMD), we observed that the $\gamma_i/\gamma/\gamma_i$ arrangement found frequently switched to another conformation characterized by a

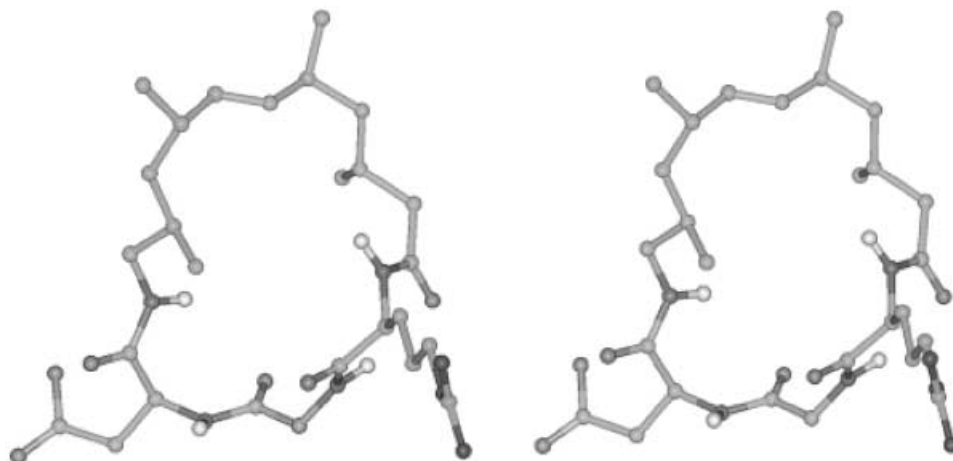


Fig. 2. Stereoview of the highest populated conformation of **4** during rMD simulation. A distinct γ_i turn at the arginine moiety and a distorted γ turn at the glycine moiety are shown.

β_{II}' -turn with Gly in the $i + 1$ position. This result is not surprising as it has been shown that Gly can substitute for a D-amino acid, and it is well-known that a D-amino acid induces a β_{II}' -turn [13]. The β_{II}' -turn found is slightly distorted, and the internal H-bond of ATUA NH with Arg CO is not populated throughout the whole rMD simulation, as shown in Table 3. During the rMD, the average distances between both H–C(α) of Gly ($i + 1$ position) and NH of ATUA ($i + 3$ position), which are thought to establish the presence of the β_{II}' -turn, are large (4.8 and 5.4 Å), and the corresponding peaks could not be observed in the ROESY plot. However, all the observed conformations are energetically accessible and fulfill all the restraints. Only the ROE peak between the NH of Asp and the NH of the ATUA is significantly violated due to the flexibility of NH of Asp (Table 4). This is also indicated by the Asp $^3J(\text{NH}, \text{H}-\text{C}(\alpha))$ coupling constant of ca. 7 Hz. Nevertheless, the $\gamma_i/\gamma/\gamma_i$ arrangement seems to be energetically favored in comparison with the β_{II}' arrangement.

The $\gamma_i/\gamma/\gamma_i$ arrangement of the RGD sequence was previously found in compound cyclo(-RGDf-N(Me)V-) by Dechantsreiter *et al.* [28]. However, the latter compound is more potent towards the $\alpha v\beta 3$ receptor than **4**. This result might be explained by the greater flexibility of cyclo(-RGD-ATUA-) (**4**). As shown by MD calculations, the β_{II}' -mimetic is not rigid enough to force the RGD sequence into the kinked conformation known to be vital for the $\alpha v\beta 3$ activity and selectivity. Moreover, additional loss of activity might be due to the lack of the aromatic residue following the RGD sequence. It has been shown that Phe following the RGD sequence, further enhances the activity [35]. Recently, Xiong *et al.* showed that, in the crystal structure of the $\alpha v\beta 3$ integrin complexed with our cyclic N(Me)-Val peptide [28], the aromatic moiety of the ligand is in close proximity and perpendicularly oriented to the aromatic ring of Tyr¹²² in the βA domain [25]. Moreover, comparison between compound **4** and cyclo(-RGDfV-) shows that the two structures differ mainly in the orientation of the Asp-CO. In the cyclo(-RGDfV-), the Asp-CO points inside, stabilizing a potential γ -turn, whereas, in **4**, the

Table 4. Distance Restraints and Their Violations from the 150-Picosecond-Restrained MD Simulation in H₂O of Cyclo(-RGD-ATUA-). Distance violations were calculated by $\langle r^{-3} \rangle^{-1/3}$ averaging.

Proton 1	Proton 2	Lower bound [Å]	Upper bound [Å]	Calculated distance [Å]	Violation [Å]
Arg NH	Arg H–C(β)	2.39	2.96	2.64 ^a	0.00
Arg NH	Arg H–C(α)	2.31	2.93	2.99	0.06
Arg NH	ATUA H–C(2)	2.15	2.94	2.48 ^a	0.00
Arg NH	ATUA CH ₃ –C(3)	4.20	5.40	4.23 ^a	0.00
Arg H–C(α)	Gly NH	2.15	2.63	2.18	0.00
Gly NH	Arg NH	3.87	4.73	4.32	0.00
Asp NH	Asp H–C(α)	2.51	3.07	3.03	0.00
Asp NH	Gly NH	3.01	4.52	4.39	0.00
Asp H–C(β)	Asp NH	2.81	3.81	2.94 ^a	0.00
ATUA NH	Asp H–C(β)	3.67	4.52	3.99 ^a	0.00
ATUA NH	Asp NH	2.35	2.97	3.30	0.33
ATUA NH	Asp H–C(α)	2.34	2.86	2.38	0.00
ATUA NH	ATUA H–C(10)	2.39	2.93	2.54	0.00
ATUA H–C(11)	ATUA CH ₃ –C(10)	2.35	3.16	2.57 ^a	0.00
ATUA H–C(10)	ATUA H _{pros} –C(9)	2.73	3.33	3.07	0.00
ATUA H–C(10)	ATUA H _{proR} –C(9)	2.31	2.83	2.52	0.00
ATUA H–C(7)	ATUA H–C(8)	2.61	3.19	3.10	0.00
ATUA CH ₃ –C(8)	ATUA H–C(7)	2.39	3.63	2.94 ^a	0.00
ATUA H–C(3)	ATUA H _{proR} –C(4)	2.24	2.74	2.55	0.00
ATUA H–C(3)	ATUA H _{pros} –C(4)	2.76	3.30	3.07	0.00
ATUA H–C(6)	ATUA H–C(5)	2.61	3.19	3.11	0.00
ATUA CH ₃ –C(3)	ATUA H–C(5)	2.69	3.29	2.93 ^a	0.00
ATUA H–C(5)	ATUA H–C(3)	3.06	3.70	3.15	0.00
ATUA H–C(6)	ATUA CH ₃ –C(5)	2.39	3.63	2.92 ^a	0.00
ATUA H–C(6)	ATUA H–C(5)	2.16	2.55	2.43	0.00
ATUA H–C(5)	ATUA H–C(6)	2.16	2.55	2.45	0.00
ATUA H–C(6)	ATUA H _{pros} –C(4)	3.60	4.49	3.81	0.00
ATUA CH ₃ –C(3)	ATUA H–C(2)	2.48	3.73	2.56 ^a	0.00

^a) Not stereospecifically assigned. For the restraint, the C-atom to which the proton is bonded to, was used.

same group points outside. As a consequence, the structure widens and the RGD sequence of **4** adopts a more-extended conformation. *Fig. 3* shows the superposition of the most populated structure of **4** with cyclo(-RGDfV-). The r.m.s.d. value for the backbone atoms of the RGD sequence is 0.9 Å.

3. Conclusions. – A large number of β -turn mimics were designed in the past. Most of them are rigidified by additional internal or external covalent linkages that mainly lead to mono- or bicyclic turn mimics. The linear turn mimic ATUA, which was investigated in our work, contains 2,4-dimethylpentane units like in polyketide natural products and the concept of allylic strain to induce a β -hairpin-like conformation. The latter concept was also used by other groups [36–38]. The ATUA was incorporated into a cyclic RGD peptide. Due to flexibility of the terminal parts of ATUA, the RGD sequence can arrange in an ensemble of different conformations that results in drastically lower biological activity and selectivity against $\alpha v \beta 3$ integrins compared to the lead peptide cyclo(-RGDfV-). Obviously, the RGD sequence is not forced by the

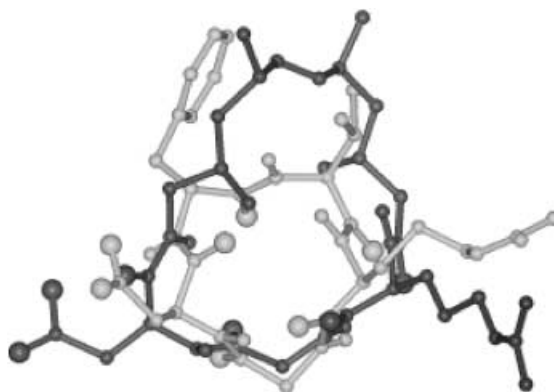


Fig. 3. Superposition of the highest populated conformation during rMD simulation of **4** (black) with cyclo(-RGDFV-) (gray).

ATUA to adopt the proper orientation of the pharmacophoric side chains. In addition, the aromatic side chain of D-Phe is missing in **4**. However, evidence was provided that a long linear molecule can adopt a β -turn-like conformation only by influence of the allylic strains and the steric hindrance of Me groups. In fact, the superposition of the ATUA in **4** with an ideal β II'-turn shows a good fit.

Experimental Part

General. Commercially available reagent-grade reagents were used without further purification. Compound **2** was synthesized in the laboratory of R. W. H. Trityl chloride polystyrol (TCP) resin (0.95 mmol/g) was purchased from *PepChem*. Coupling reagents and amino acid derivatives were purchased from *Advanced ChemTech* and *NovaBiochem*. Flash chromatography (FC): silica gel 60 (230–400 mesh ASTM) from *Merck*. NMR Experiments: *Bruker* spectrometers (*DMX-500*, *DMX-750*). Mass spectra: electrospray ionization (ESI); *LCQ-Finnigan* instrument.

(3R,5S,6E,8S,10R)-11-[(9H-Fluoren-9-ylmethoxy)carbonyl]amino-3,5,8,10-tetramethylundec-6-enoic Acid (Fmoc-ATUA; **3**). Ester **2** (150 mg, 0.482 mmol) was refluxed in conc. KOH soln. (6 ml) for 4 h. After cooling to r.t., the pH was adjusted to 7.5 by adding conc. HCl soln. and NaHCO₃ (50 mg). After addition of acetone (6 ml) and *N*-{[(9H-fluoren-9-ylmethoxy)carbonyl]oxy}succinimide (Fmoc-OSu; 250 mg), the mixture was stirred overnight at r.t. Subsequently, the acetone was evaporated, and the mixture acidified with 2N HCl to pH 2 and extracted with AcOEt. The org. phase was dried (MgSO₄) and evaporated and the residue (410 mg) purified by FC (SiO₂ (75 g), hexane/AcOEt 4 : 1 with 1% AcOH): **3** (90 mg, 39%; purity > 95% by HPLC). Slightly yellow oil. ¹H-NMR (500 MHz, CDCl₃); ¹H-TOCSY, ¹H-DQF-COSY, ¹³C,¹H-HSQC): 7.76 (*d*, *J* = 7.4, 2 arom. H (Fmoc)); 7.59 (*d*, *J* = 7.4, 2 arom. H (Fmoc)); 7.39 (*t*, *J* = 7.4, 2 arom. H (Fmoc)); 7.31 (*t*, *J* = 7.4, 2 arom. H (Fmoc)); 5.10–5.15 (*m*, NH); 5.07–5.12 (*m*, H–C(6), H–C(7)); 4.41 (*d*, *J* = 6.7, CHCH₂OCON); 4.21 (*t*, *J* = 6.8, CHCH₂OCON); 3.00–3.09, 2.93–3.00 (*2m*, 2 H–C(11)); 2.25, 2.16 (*2m*, 2 H–C(2)); 2.14 (*m*, H–C(5), H–C(8)); 1.94 (*m*, H–C(3)); 1.62 (*m*, H–C(10)); 1.23, 1.10 (*2m*, 2 H–C(4)); 1.23, 1.01 (*2m*, 2 H–C(9)); 0.97 (*d*, *J* = 7.0, Me–C(5), Me–C(8)); 0.90 (*d*, *J* = 7.0, Me–C(3)); 0.85 (*d*, *J* = 7.0, Me–C(10)). ¹³C-NMR (125 MHz, CDCl₃): 176.9 (CO); 156.9 (CO(Fmoc)); 144.0 (arom. C (Fmoc)); 141.3 (arom. C (Fmoc)); 135.0 (C(6), C(7)); 128.1 (arom. CH (Fmoc)); 127.3 (arom. CH (Fmoc)); 125.3 (arom. CH (Fmoc)); 120.3 (arom. CH (Fmoc)); 66.9 (CHCH₂OCON); 47.9 (C(11)); 47.6 (CHCH₂OCON); 44.6 (C(4)); 42.3 (C(2)); 42.1 (C(9)); 35.0 (C(5); C(8)); 32.0 (C(10)); 28.5 (C(3)); 22.4 (Me–C(5), Me–C(8)); 19.4 (Me–C(3)); 17.2 (Me–C(10)). ESI-MS: 478.2 ([*M* + H]⁺), 977.5 ([2*M* + Na]⁺), 993.5 (2*M* + K)⁺. HPLC (*Amersham Pharmacia*, *YMC-RP*, 4.6 mm × 250 mm, 5 μm C₁₈; 1 ml/min, 30 min linear gradient 50–100% *B*; eluent *A* H₂O (0.1% CF₃COOH), eluent *B* MeCN (0.1% CF₃COOH), 220-nm UV detector): *t*_r 23.24 min.

Peptide Synthesis of Cyclo(-RGD-ATUA-)(4). The peptide was synthesized by solid-phase peptide synthesis (SPPS) [39][40] on the trityl chloride polystyrol (TCP resin) [41][42] according to the Fmoc strategy [43][44]. The resin was loaded with **3**. Subsequently, Fmoc-Asp(O^tBu), Fmoc-Gly, and Fmoc-Arg(Pbf) (Pbf = 2,2,4,6,7-pentamethyldihydrobenzofuran-5-sulfonyl) were coupled with *O*-(1*H*-benzotriazol-1-yl)-*N,N,N,N'*-tetramethyluronium tetrafluoroborate (TBTU), 1-hydroxy-1*H*-benzotriazole (HOBt) in 3-fold excess and ³Pr₂NEt as base and 1-methylpyrrolidin-2-one (NMP) as solvent. The Fmoc deprotection between the couplings and at the end of the sequence was done with 20% piperidine in NMP. The peptide was cleaved from the resin by treatment with 20% 1,1,1,3,3,3-hexafluoro-propan-2-ol (HFIP) in CH₂Cl₂. Cyclization was performed *via in situ* activation with diphenoxyphosphoryl azide (DPPA) and with NaHCO₃ as solid base under high-dilution conditions in DMF for 16 h [45]. For side-chain deprotection, the cyclic peptide was treated with a soln. of 95% CF₃COOH, 2.5% H₂O and 2.5% ³Pr₂SiH for 3 h at r.t. The crude peptide was purified by prep. HPLC (*Amersham Pharmacia, YMC-RP*, 30 mm × 250 mm, 5 μm C₁₈; 25 ml/min, 30 min linear gradient 30–70% *B*; eluent *A* H₂O (0.1% CF₃COOH), eluent *B* MeCN (0.1% CF₃COOH), 220-nm UV detector). ESI-MS: 566.5 ([*M* + *H*]⁺).

NMR Spectroscopy of Cyclo(-RGD-ATUA-)(4). Sample: 0.6 mg of **4** dissolved in 500 μl of solvent (H₂O/D₂O 90:10 (v/v)) yielded a sample concentration of 2 mmol/l. Solvent-signal suppression was achieved by the WATERGATE scheme [46]. 1D-NMR (*DMX-750*): 32K data points, 8 scans, 1.5 s relaxation delay; temperature coefficients of amide protons: seven 1D experiments were acquired in a temp. range from 283 to 308 K (5-K steps). DQF-COSY (*DMX-750*): acquisition: 2K (*t*₂) × 768 (*t*₁) data points, 16 scans per *t*₁ increment, 2.0 s relaxation delay; processing: squared cosine as window function in both dimensions, zero filling and FT to 2K × 1K real/real data points. ¹³C-HSQC (*DMX-750*): acquisition: 1K (*t*₂) × 186 (*t*₁) data points, 8 scans per *t*₁ increment, 1.5 s relaxation delay, ¹³C-GARP decoupling during *t*₂; processing: squared cosine as window function in both dimensions, zero filling and FT to 2K × 512 real/real data points. TOCSY (*DMX-500*): acquisition: 2K (*t*₂) × 512 (*t*₁) data points, 8 scans per *t*₁ increment, 2.0 s relaxation delay, isotropic mixing with DIPSI-2, 40 ms mixing time, 8.3 kHz spinlock field; processing: squared cosine as window function in both dimensions, zero filling and FT to 2K × 1K real/real data points. ROESY (*DMX-500*): acquisition: 2K (*t*₂) × 256 (*t*₁) data points, 64 scans per *t*₁ increment, 1.5 s relaxation delay, 200 ms mixing time, 4.7 kHz spinlock field; processing: squared cosine as window function in both dimensions, zero filling and FT to 2K × 1K real/real data points.

Computer Simulations. The structure calculations were performed on *Origin-200* computers. Metric matrix distance geometry calculations were carried out with a modified [30] version of DISGEO [31][32]. The DG procedure started with the embedding of 100 structures by random metrization [47]. For the refinement of the structures, DISGEO employs distance- and angle-driven dynamics with NOE restraints and an additional ³*J*-coupling potential [30] according to the *Karplus* equation. The MD calculations were carried out with the program DISCOVER and the CVFF force field [48]. The best structure resulting from DG calculation was placed in a cubic box with a box length of 40 Å and soaked with H₂O. The calculations were done with the explicit-image model of periodic boundary conditions. After energy minimization by steepest descent and conjugate gradient, the system was heated gradually starting from 10 K and increasing to 50, 100, 150, 200, 250, and 300 K in 1-ps steps, each by direct scaling of velocities. The system was equilibrated for 25 ps with temperature bath coupling (300K). Configurations were saved every 100 fs for another 150 ps. The free MD simulation started from the end of the restrained MD.

The authors gratefully acknowledge technical assistance from *M. Kranawitter* and *B. Cordes*. We wish to thank *G. Voll* and *E. Locardi* for useful advice and *Merck KGaA* for performing the screening assays. Financial support was provided by the *Deutsche Forschungsgemeinschaft* and the *Fonds der Chemischen Industrie*.

REFERENCES

- [1] G. D. Rose, L. M. Gierasch, J. A. Smith, *Adv. Protein Chem.* **1985**, *37*, 1.
- [2] J. B. Ball, P. F. Alewood, *J. Mol. Recogn.* **1990**, *3*, 55.
- [3] K. Burgess, *Acc. Chem. Res.* **2001**, *34*, 826.
- [4] J. Venkatraman, S. C. Shankaramma, P. Balaram, *Chem. Rev.* **2001**, *101*, 3131.
- [5] K. D. Stigers, M. J. Soth, J. S. Novick, *Curr. Opin. Chem. Biol.* **1999**, *3*, 714.
- [6] S. Hanessian, G. McNaughton-Smith, H.-G. Lombart, W. D. Lubell, *Tetrahedron* **1997**, *53*, 12789.
- [7] U. Egner, A. Müller-Fahrnow, E. Eckle, *Pestic. Sci.* **1997**, *51*, 95.
- [8] U. Schopfer, M. Stahl, T. Brandl, R. W. Hoffmann, *Angew. Chem., Int. Ed.* **1997**, *36*, 1745.

- [9] F. Johnson, *Chem. Rev.* **1968**, *68*, 375.
- [10] R. W. Hoffmann, *Chem. Rev.* **1989**, *89*, 1841.
- [11] R. W. Hoffmann, *Angew. Chem., Int. Ed.* **1992**, *31*, 1124.
- [12] R. Haubner, W. Schmidt, G. Hölzemann, S. L. Goodman, A. Jonczyk, H. Kessler, *J. Am. Chem. Soc.* **1996**, *118*, 7881.
- [13] M. Koppitz, M. Huenges, R. Gratias, H. Kessler, S. L. Goodman, A. Jonczyk, *Helv. Chim. Acta* **1997**, *80*, 1280.
- [14] E. Lohof, E. Planker, C. Mang, F. Burkhart, M. A. Dechantsreiter, R. Haubner, H.-J. Wester, M. Schwaiger, G. Hölzemann, S. L. Goodman, H. Kessler, *Angew. Chem., Int. Ed.* **2000**, *39*, 2761.
- [15] M. Aumailley, M. Gurrath, G. Müller, J. Calvete, R. Timpl, H. Kessler, *FEBS Lett.* **1991**, *291*, 50.
- [16] M. Pfaff, K. Tangemann, B. Müller, M. Gurrath, G. Müller, H. Kessler, R. Timpl, J. Engel, *J. Biol. Chem.* **1994**, *269*, 20233.
- [17] G. Müller, M. Gurrath, H. Kessler, R. Timpl, *Angew. Chem., Int. Ed.* **1992**, *31*, 326.
- [18] R. Haubner, R. Gratias, B. Diefenbach, S. L. Goodman, A. Jonczyk, H. Kessler, *J. Am. Chem. Soc.* **1996**, *118*, 7461.
- [19] E. Ruoslahti, M. D. Pierschbacher, *Cell* **1986**, *44*, 517.
- [20] R. O. Hynes, *Cell* **1987**, *48*, 549.
- [21] E. Ruoslahti, M. D. Pierschbacher, *Science (Washington, D.C.)* **1987**, *238*, 491.
- [22] T. A. Springer, *Nature (London)* **1990**, *346*, 425.
- [23] R. O. Hynes, *Cell* **1992**, *69*, 11.
- [24] A. van der Flier, A. Sonnenberg, *Cell Tissue Res.* **2001**, *305*, 285.
- [25] J. P. Xiong, T. Stehle, R. G. Zhang, A. Joachimiak, M. Frech, S. L. Goodman, M. A. Arnaout, *Science (Washington, D.C.)* **2002**, *296*, 151.
- [26] P. C. Brooks, A. M. P. Montgomery, M. Rosenfeld, R. A. Reisfeld, T. H. Hu, G. Klier, D. A. Cheresch, *Cell* **1994**, *79*, 1157.
- [27] S. Strömblad, D. A. Cheresch, *Chem. Biol.* **1996**, *3*, 881.
- [28] M. A. Dechantsreiter, E. Planker, B. Mathä, E. Lohof, G. Hölzemann, A. Jonczyk, S. L. Goodman, H. Kessler, *J. Med. Chem.* **1999**, *42*, 3033.
- [29] G. A. G. Sulyok, C. Gibson, S. L. Goodman, G. Hölzemann, M. Wiesner, H. Kessler, *J. Med. Chem.* **2001**, *44*, 1938.
- [30] D. F. Mierke, H. Kessler, *Biopolymers* **1993**, *33*, 1003.
- [31] T. F. Havel, *Prog. Biophys. Mol. Biol.* **1991**, *56*, 43.
- [32] T. F. Havel, Quantum Chemistry Program, Exchange No. 507, Indiana University, 1988.
- [33] E. Osawa, T. Ouchi, N. Saito, M. Yamato, O. S. Lee, M. K. Seo, *Magn. Reson. Chem.* **1992**, *30*, 1104.
- [34] K. Imai, E. Osawa, *Magn. Reson. Chem.* **1990**, *28*, 668.
- [35] L. Tranqui, A. Andrieux, G. Hudry-Clergeon, J.-J. Ryckewaert, S. Soye, A. Chapel, M. H. Ginsberg, E. F. Plow, G. Marguerie, *J. Cell. Biol.* **1989**, *108*, 2519.
- [36] P. Wipf, T. C. Henninger, S. J. Geib, *J. Org. Chem.* **1998**, *63*, 6088.
- [37] R. R. Gardner, G.-B. Liang, S. H. Gellman, *J. Am. Chem. Soc.* **1995**, *117*, 3280.
- [38] R. R. Gardner, G.-B. Liang, S. H. Gellman, *J. Am. Chem. Soc.* **1999**, *121*, 1806.
- [39] R. B. Merrifield, *J. Am. Chem. Soc.* **1963**, *85*, 2149.
- [40] R. B. Merrifield, *Angew. Chem., Int. Ed.* **1985**, *24*, 799.
- [41] K. Barlos, D. Gatos, J. Kallitsis, G. Papahotiu, P. Sotiriu, W. Q. Yao, W. Schäfer, *Tetrahedron Lett.* **1989**, *30*, 3943.
- [42] K. Barlos, O. Chatzi, D. Gatos, G. Stavropoulos, *Int. J. Pept. Protein Res.* **1991**, *37*, 513.
- [43] L. A. Carpino, G. Y. Han, *J. Am. Chem. Soc.* **1970**, *92*, 5748.
- [44] G. B. Fields, R. L. Noble, *Int. J. Pept. Protein Res.* **1990**, *35*, 161.
- [45] S. F. Brady, W. J. Paleveda, B. H. Arison, R. M. Freidinger, R. F. Nutt, D. F. Veber, 'Proceedings of the 8th American Peptide Symposium', Ed. V. J. Hruby, D. H. Rich, *Pierce Chemical Company*, Rockford IL, 1983, p. 127.
- [46] M. Piotto, V. Saudek, V. Sklenár, *J. Biomol. NMR* **1992**, *2*, 661.
- [47] T. F. Havel, *Biopolymers* **1990**, *29*, 1565.
- [48] A. T. Hagler, S. Lifson, P. Dauber, *J. Am. Chem. Soc.* **1979**, *101*, 5122.

Received June 8, 2002